# Integration of Multiple Motion Vectors Over Space: An fMRI Study of Transparent Motion Perception

Lars Muckli,* Wolf Singer,* Friedhelm E. Zanella,† and Rainer Goebel*,‡

*Max Planck Institute for Brain Research, Neurophysiology, 60528 Frankfurt am Main, Germany; †Department of Neuroradiology, Johann Wolfgang Goethe-University, 60528 Frankfurt am Main, Germany; and ‡Department of Psychology, Neurocognition, University Maastricht, 6200MD Maastricht, The Netherlands

**Visual scenes are frequently composed of objects that move in different directions. To segment such scenes into distinct objects or image planes, local motion cues have to be evaluated and integrated according to criteria of global coherence. When several populations of coherently moving random dots penetrate each other, the visual system tends to assign them to different planes—perceived as transparent motion. This process of integration was studied by changing the angle of motion trajectories with which groups of dots penetrate each other or by varying the spatial constellation of dots moving in opponent directions. Psychophysical testing revealed that stimuli providing almost identical local motion cues could be perceived in three very different ways: (1) as a matrix of stationary flickering dots, (2) as a single surface of coherently moving dots, and (3) as two transparent dot matrices moving in different directions. Behaviorally controlled functional magnetic resonance imaging (fMRI) was used to identify brain regions that contribute to the integration of local motion cues into coherently moving surfaces. Activation of the human motion complex (hMT+/V5) and of areas in the fusiform gyrus (FG) as well as in the intraparietal sulcus (IPS-occ) was correlated with the perception of coherent motion and especially hMT+/V5 took a central role in differentiating transparent motion from single-surface coherent motion.** © 2002 Elsevier Science (USA)

*Key Words:* fMRI; motion perception; transparent motion; motion opponency; vision; hMT+/V5.

## INTRODUCTION

Coherent movement of random dots is commonly perceived as motion of a single textured surface. If two superimposed random dot patterns move in different directions, the visual system represents two surfaces (Wallach and O'Connell, 1953). Surfaces that share the same region of visual space without occluding one another are consistently perceived as two transparent surfaces, each defined by a set of dots, moving continuously and independently across each other (Gibson *et al.,* 1959). If additional segmentation cues are available, i.e. contrast, color or binocular disparity (Adelson and Movshon, 1982; Krauskopf and Farell, 1990; Qian, 1997), it is possible to perceive several transparent surfaces in the same region of the visual field. However, in the typical laboratory condition where coherently moving populations of randomly spaced dots are used, no more than two moving surfaces can be perceived simultaneously (Andersen, 1989; Mulligan, 1992). In order to evoke the percept of transparent motion, coherently moving dots need to be bound together perceptually and assigned to the same surface, implying segregation of dots that move in different directions, even if they are closely spaced. Yet this mechanism gets compromised if every dot that moves in one direction is precisely paired for the time of movement by a nearby dot that is moving in the opposite direction (Qian *et al.,* 1994a). In such paired conditions perception of coherent motion vanishes for either set of dots. This effect has been used to study the visual processes that enable transparent motion perception, and it has been used to identify transparent motion sensitive neurons in the monkey visual cortex (Qian and Andersen, 1994; Heeger *et al.,* 1999). Responses of the neurons that are involved in segregating different motion vectors must not be compromised by other nearby dots that move in the opposite direction. In other words, the receptive fields of the neurons evaluating the motion cues must be smaller than the distance between oppositely moving dots so that their responses do not get antagonized. Direction selective cells with these properties have been found in the primary visual cortex (area V1) of monkeys (Snowden *et al.,* 1991; Qian and Andersen, 1994). Surprisingly, however, neurons in V1 preserve uncompromised responses even at dot distances that are so small that transparent motion is no longer perceived. This indicates that the binding process that mediates the association of coherently moving dots to distinct surfaces operates at a different spatial scale, i.e., with lower

spatial resolution than the segregation process that extracts the motion cues, suggesting that the binding function is achieved by another cortical area. Since the responses of neurons in monkey MT/V5 have been shown to change when modifications in the distance between oppositely moving dots lead to perceptual changes (Qian and Andersen, 1994; Heeger *et al.,* 1999), it is likely that the binding function is realized in this cortical area.

Our study is designed to investigate in detail, which areas participate in the cortical network that is responsible for this type of motion integration. Two parameters in the dot displays were systematically varied in order to induce different percepts on the basis of almost identical local motion cues. The orientation of motion trajectories was varied in order to induce either the perception of one coherently moving surface or two transparently moving surfaces. Small orientation differences led to the percept of coherent motion, large differences to transparent motion. The vicinity of oppositely moving dots was varied to induce the percept of either transparent motion or the perception of a nonmoving pattern.

Perceptual thresholds were obtained prior to the fMRI experiments and were in addition controlled during one of the fMRI experiments. Blood oxygenation level dependent (BOLD) changes were related to changes in the perceptual condition. Brain activity related to transparent motion perception was cross-validated under passive viewing conditions.

## MATERIALS AND METHODS

### Subjects

Two psychophysical experiments (PI and PII) and two fMRI experiments (fMRI-a and fMRI-b) were performed. Ten subjects (8 males, 2 females, age range: 25–35 years) participated in the psychophysical studies (PI: 4; PII: 6) and 14 subjects (8 males, 6 females, age range: 25–35 years) in the functional imaging studies (7 each fMRI experiment). Four subjects that participated in the fMRI-b participated also in the psychophysical studies (PI: 2; PII: 2). All subjects had normal or corrected to normal vision, had no neurological history and had given their informed consent.

### Viewing Conditions

The stimuli were computer generated (Digital DECpc Celebris XL 590, Digital Equipment, Munich, Germany) using a special graphics adapter (ELSA Winner 2000 Pro/X) and the Elsa Powerlib C library. In the fMRI experiments stimuli were projected onto a frosted screen with an LCD projector (EIKI LC-6000, Eiki GmbH, Idstein, Germany; graphic resolution $640 \times 480$ pixels; vertical refresh rate 60 Hz). Subjects

viewed the screen through a mirror mounted to the head coil. The visual field size was $17° \times 12°$ (fMRI-a) and $29° \times 22°$ (fMRI-b). The dot size was 2′ 50″ (fMRI-a and fMRI-b).

Psychophysical experiments (PI and PII) were similar in most respects but the stimuli were presented with different graphical resolutions. The viewing conditions of the PI experiment (viewing distance: 0.75 m) and the fMRI-b experiment (viewing distance 1.30 m) were matched precisely to the same stimulus size and spatiotemporal dot parameters (field size: $29° \times 22°$, dot size: 2′ 50″, dot velocity: $2.8°$ s$^{-1}$). In the PI experiment a low graphic resolution mode ($640 \times 480$ pixels; vertical refresh rate: 60 Hz; 21 inch monitor, Hitachi Accuvue, HM 4921-D) was used to deliver the stimuli. The PII experiment was designed to test the stimuli on a finer spatial scale. Therefore the graphical resolution and the viewing distance were increased for PII ($1152 \times 864$ pixels; refresh rate: 130 Hz, viewing distance 2 m, same monitor) so that the size of the stimuli and their components were markedly reduced (visual field size: $10° \times 10°$, dot size: 40″, dot velocity: $2°$ s$^{-1}$).

### Stimuli

Stimuli consisted of randomly distributed pairs of dots. In the fMRI-a experiment the angle between the dots of a pair was varied (see below, and Figs. 1a and 1b). No behavioral responses were requested during fMRI-a. In PI, PII, and fMRI-b the dots of a pair moved in opposite directions and contained a target region. Target regions were located in one of the four quadrants of the stimuli (Fig. 1d) and were defined by a contrast of motion directions. Dots within the target region moved along trajectories orthogonal to those of the background. The subjects ability to locate the target was examined as a function of the distance between the paired dots.

### Stimuli for fMRI-a

In the fMRI-a experiment the angles between the motion trajectories of dot pairs were varied in a parametric design. Stimuli consisted of 24 pairs of moving white dots (dot pair density: 0.5/deg$^2$). The distance of the dots at the mid point of the motion trajectory and the stretch of paired moving dots were set to a constant value of 54′. Angles varied between 0°, 23°, 62°, 90°, 118°, and 180°. The two motion trajectories were oriented symmetrically around the left downwards diagonal (polar angle: $-\pi 3/4$; see Figs. 1a and 1b). These angles were selected because they could be generated on a computer screen with pixel wise displacements that resulted in approximately the same velocities: 11.8°, 10.1°, 11.5°, 11.2°, 11.5°, 11.8°/s. Note that the two simultaneously presented motion fields always moved with the same speed and only varied between trials with respect to the angle of the motion trajecto-
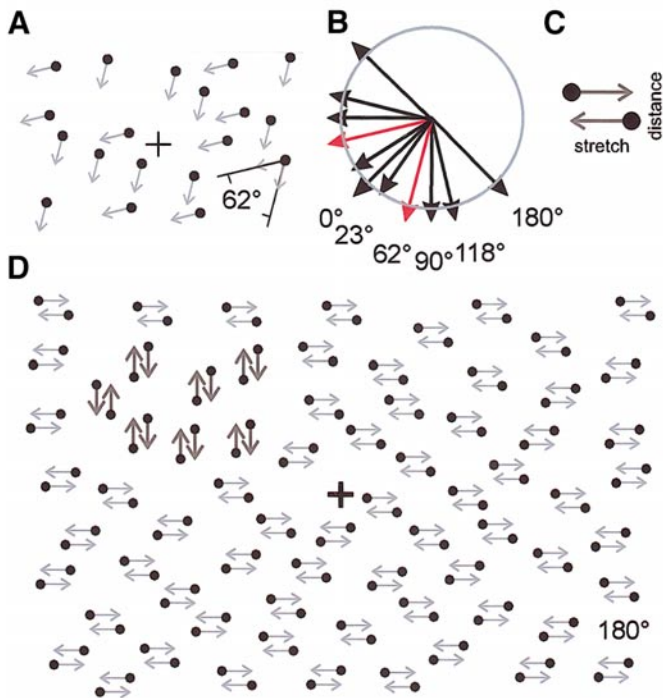
**FIG. 1.** Transparent motion stimuli consist of two groups of random dot patterns that move in different directions. For the example shown in (A), the motion trajectories of the two groups differs by an angle of 62°. (B) In the fMRI-a experiment 6 different motion angles of motion trajectories were used (0°, 23°, 62°, 90°, 118°, and 180°). The motion trajectories were oriented around the left downwards diagonal and resulted in approximately the same velocities (indicated by the length of the arrows). (D) Opponent moving dot displays consisted of randomly distributed pairs of dots that moved in opposite directions. The stimulus is a variation of the 'paired' transparent motion display used by Kolb and Braun (1995) and Qian et al. (1994a). Target regions are defined by the contrast in motion direction. Dots within the target region (shown in the left upper quadrant) move along trajectories that are orthogonal to the surrounding background. (C) The perception of the display depends on the vicinity of dots moving in opponent directions. Vicinity can be varied along the motion direction (stretch) and orthogonal to the motion direction (distance). Both of these parameters were varied during psychometric testing. Only the distance was changed during the fMRI scanning.

ries. Blocks lasted for 16 s and were presented interleaved with displays of stationary random dot patterns (48 dots) or fixation. The protocol consisted of three repetitions of a 16-s-long sequence consisting of: fixation, static, TM-0°, static, TM-23°, static, TM-62°, static, TM-90°, static, TM-118°, static, TM-180°, static, fixation. Subjects performed two runs of the same protocol with fixation conditions replacing the static ones in one half of the runs.

### Stimuli for P I and P II

Pairs of white dots move on dark backgrounds (PI: 300 pairs, dot pair density 0.5/deg²/PII: 500 pairs, dot pair density: 5/deg²). Each pair consisted of two nearby

dots that appeared simultaneously, moved towards one another, passed each other and disappeared. In the next frame, the pair was presented at another randomly selected screen position, starting the same sequence.

The perception of motion transparency depends on the spatiotemporal relation between the oppositely moving dots (Qian et al., 1994a). We varied two spatiotemporal stimulus parameters: the stretch along the motion direction (others refer to it as dot-lifetime; see Qian et al., 1994a; Kolb and Braun, 1995) and the distance of dots orthogonal to the motion direction (Fig. 1c). Stretch and distance are combined to a vicinity ratio, the ratio of dot distance over dot stretch, which will be used below as a measure to account for both parameters simultaneously. For each experiment the stretch was varied in five steps and ranged over both experiments between 2.1′ and 59′ (PI: 8.4′, 14′, 19.6′, 25.2′, 58.8′/PII: 2.1′, 3.5′, 4.9′, 6.3′, 14.7′). The distance ranged over both experiments between 0.7′ and 25′ (PI: 2.8′, 5.6′, 8.4′, 14′, 25.2′/PII: 0.7′, 1.4′, 2.1′, 3.5′, 6.3′). Target regions (size PI: 4.4° × 5.3°/PII:2° × 2°) were centered in one of the four quadrants of the display (vertical eccentricity PI: 4.4°/PII: 1.5°, horizontal eccentricities: PI: 1.1°/PII: 1.5°). In PI the motion trajectories were oriented along the main axes in PII along the main diagonals.

### Stimuli for fMRI-b

Two stimulus conditions from PI experiment were used for fMRI-b measurements. The stimuli consisted of 300 pairs of oppositely moving white dots (visual field size 29° × 22°, dot size: 2′ 50″, dot velocity: 2.8° s, dot pair density: 0.5/deg²). The stretch was kept constant at a value of 19.6′, which led also to a constant duty cycle of 8.3 Hz. Distance was varied between two values, 8′ and 25′. From the PI experiment it was evident that this change in distance would suffice to create two distinct conditions of opponent motion. With a distance value of 25′ displays were perceived as transparently moving dot displays (TM), while with a distance of 8′, displays were perceived as static incoherent flicker (nontransparent: NT). In the latter displays, targets defined by motion contrasts were not detected.

During fMRI scanning TM and NT displays were presented in blocks of 32 s (equal to 8 scans of a brain volume covered by 15 slices). Within a block, targets appeared and disappeared at random intervals (mean inter target interval: 2.5 s; mean target presentation time 3.5 s). The time required for a build up of a target was 120 ms, as it takes the duration of a dot life cycle until every dot pair has been exchanged. Targets appeared randomised in the left or right lower visual field with a strong bias (85%) toward one hemifield. The preferred hemifield changed between blocks of presen-
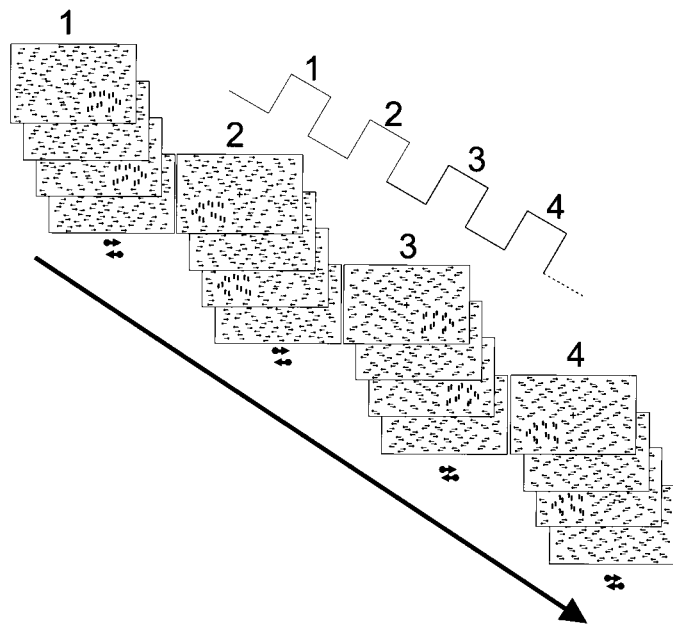
**FIG. 2.** Procedure of fMRI-b experiment. Experimental conditions change after blocks of 32 s between opponent motion conditions (1, 2, 3, 4) and fixation conditions. Displays of TM (1, 2) and NT (3, 4) are identical in local motion vectors but the distance of opponent moving vectors is reduced in the NT conditions. Targets appeared and disappeared at random intervals in the left or right lower visual field with a strong tendency (85%) to one hemifield. The preferred hemifield changed between blocks of presentation (left in 1 and 3; right in 2 and 4). The fMRI-b experiment consisted of four repetitions of this sequence.

tation. Conditions with preferred left or right target presentation and TM or NT conditions were alternated and presented interleaved with periods of fixation. A fixation cross was present during all conditions and was the only stimulus during the fixation condition. (Protocol consisted of four repetitions of: TM-left, TM-right, NT-right, NT-left; see Fig. 2).

### The Task

In the fMRI-a experiment subjects were instructed to attend to the stimulus while maintaining fixation on a small white cross in the center of the screen.

In the psychophysical experiments stimuli were presented for 250 ms. Subjects were asked to guess the location of the target in one of four quadrants of the display (four-alternative forced-choice testing, subjects entered their selection with the right hand on a number key pad in which the position of the numbers matched analogously to the position of the targets: 4, left-upper; 5, right-upper; 2, right-lower; 1, left-lower) and rate their confidence subsequently using categories one to four (indicated by pressing one of four adjacent keys accessible with the left hand on a German PC keyboard: y, x, c, v). At least 870 trials were performed by each subject. A small number of catch trials

were presented in some selected conditions. Catch trials contained no targets and allowed the assessment of the baseline for confidence ratings.

In the fMRI-b experiment subjects were instructed to maintain fixation on a small white cross, which was present in the center of the screen throughout all conditions, and to respond to every onset of a target by indicating its location with the left or right response button (for left and right target presentation). Offset of the target was indicated by releasing the response button. Fixation was controlled during the experiment in two subjects using a MRI compatible infrared eye-recording device (Ober2, Permobil Meditech AB, Timrà, Sweden).

### Image Acquisition

Echoplanar images were collected on an 1.5-T scanner (Siemens Magnetom Vision, Siemens, Erlangen, Germany) using the standard head coil and the Siemens Magnetom gradient overdrive. We used a gradient echo echoplanar sequence (TR = 4000 ms; TE = 69 ms; FA = 90°) to visualize changes of BOLD (blood oxygen level dependent) contrast (FOV = 200–220 mm$^2$, slice thickness = 4 mm, imaging matrix = 128 × 128; resulting voxel size = ca. $1.6 \times 1.6 \times 4$ mm$^3$). Images were acquired in 15 contiguous slices oriented approximately in parallel to the calcarine fissure. A T1-weighted 3-D magnetization prepared rapid acquisition gradient echo sequence (MP RAGE) scan (voxel size = $1.0 \times 1.0 \times 1.0$ mm$^3$) lasting 8 min was recorded in the same session as the functional measurements. Additional T1-weighted 3-D data sets tuned to optimize the contrast between gray and white matter were recorded in separate recording sessions lasting 24 min.

### Data Analysis

*Analysis of psychophysical data.* Performance in target location and subjective confidence ratings were correlated for each subject and each stimulus condition. Performance and confidence ratings were plotted as a function of stimulus conditions. Stimulus conditions were expressed as the ratio of motion stretch over dot distance. Individual psychophysical data were incorporated in a group analysis.

During fMRI-b experiment responses were considered to be correct if the subjects indicated the correct side of the target (left or right) within 3 s after appearance and with release of the button within 3 s after disappearance of the target. 100% performance would include the correct detection of all on- and offsets. The chance level for onset detection is 25% correct onset responses (leaving the offset response unconsidered).

*fMRI data analysis.* Data analysis including preprocessing (3-D motion correction, spatial and temporal smoothing, linear trend removal), correlation analyses (using the general linear model for multiple

regressions), 3-D transformation into the coordinate system of Talairach and Tournaux (1988), surface rendering, cortex inflation, and cortex flattening were performed using BrainVoyager 4.4 software, which is described in more detail elsewhere (Dierks *et al.,* 1999; Kriegeskorte and Goebel, 2001; Goebel *et al.,* 1998; Linden *et al.,* 1999).

Prior to statistical analysis functional images were temporally smoothed using a FFT based band-pass filter. 2-D images were then transformed into the 3-D structural data set and interpolated to the same resolution (voxel size = $1.0 \times 1.0 \times 1.0$ mm$^3$). Since the 2-D functional maps and 3-D structural measurements were performed within the same recording session, coregistration of the respective data sets could be computed directly relating the Siemens slice position parameters of the T2*-weighted images and the T1-weighted 3-D MP RAGE measurements to the initial overview (scout). For each subject the structural 3-D and functional 4-D data sets were transformed into Talairach space (Talairach and Tournaux, 1988), which allows to compare activated brain regions across different experiments and across different subjects and to determine Talairach coordinates of activated regions. The Talairach transformation was performed using the manually specified location of the anterior and the posterior commissure (AC, PC, to align the stereotaxic axes) and the extreme points of the cerebrum to perform a piecewise affine and continuous transformation for each of the 12 defined subvolumes. The transformed functional data were then smoothed in 3-D space with a Gaussian filter (FWHM = 3 mm) and corrected for head movements with subvoxel precision (translation and rotation parameters of rigid body transformations relative to third volume). Movement corrections were less than 0.25 mm in all subjects.

In order to evaluate statistically the differences between the experimental conditions we used a multiple regression approach. In the fMRI-a experiment the stimulation protocols for the different motion trajectories were used in a six-predictor model (TM-0°, TM-23°, TM-62°, TM-90°, TM-118°, TM-180°). Each stimulation protocol served to obtain appropriate reference functions reflecting experimental and baseline conditions, respectively (experimental condition = 1, baseline condition = 0). The stimulation protocols were convoluted with a hemodynamic response function (Boynton *et al.,* 1996) to account for the expected delay and devolution of the BOLD signal. These reference functions served as independent predictors for a general linear model (GLM). At each location (106720 voxels in Talairach space), the amount of explained variance was tested for significance using $F$ statistics. $P$ values were corrected for multiple comparisons using Bonferroni correction over all (106720) voxels. Only Bonferroni corrected $P$-values are indicated as corrected. For statistical comparisons between the experimental conditions the mean value for each condition was approximated by the beta weights of the GLM model. For the analysis of systematic changes in relation to the increasing angles in fMRI-a experiment, beta weights were correlated to the angles of the TM conditions ($r$ and $P$ values). Contrast maps were calculated on the basis of the GLM model (beta weights) and tested for significance using $t$ statistics.

In the fMRI-b experiment the stimulation protocol for TM and NT served to obtain appropriate reference functions. These reference functions served as independent predictors for a general linear model (GLM). The proportion of variance explained by the model was tested for significance using $F$ statistics (ANOVA). If $P$ values are indicated to be corrected for multiple comparisons, a Bonferroni correction over all 106720 voxels has been performed. Contrast maps were calculated by comparison of the estimated beta-weights and are tested for significance by $t$ statistics.

The same data were also analyzed with a four predictor GLM to account for the left and right target presentation (TM-right, TM-left, NT-right, NT-left). Multiple correlation maps and contrast maps were superimposed on the T1-weighted 3-D anatomical reference scans. For the visualization of group data we used the individual MNI template brain (template provided with courtesy of the Montreal Neurological Institute).

The individual brain surfaces and the template brain were reconstructed based on the high-resolution T1-weighted structural 3-D recordings. The white/gray matter boundary was segmented, reconstructed, smoothed, morphed and flattened as described in detail elsewhere (Dierks *et al.,* 1999; Kriegeskorte and Goebel, 2001). A morphed surface always possesses a link to the folded reference mesh so that functional data can be shown at the correct location of partially inflated as well as flattened representations.

For a precise delineation of early visual areas in the single subject analysis, we used retinotopic maps generated in separate experiments (Engel *et al.,* 1994; Goebel *et al.,* 1998; Sereno *et al.,* 1995). Twelve contiguous slices were obtained approximately in parallel to the calcarine fissure (TR = 3000, voxel size = $1.6 \times 1.6 \times 3$ mm$^3$) and subjects were stimulated with slowly expanding checkerboard rings and slowly rotating ray shaped checkerboards from which eccentricity maps and polar angle maps were gained (for details see Goebel *et al.,* 1998). From the combination of eccentricity and polar maps we estimated field sign maps as described by Sereno *et al.* (1995) to delineate early visual areas.

## RESULTS

### Psychophysics

The perception of the dot displays changed substantially when dot distance was varied. Subjective reports and measurements of target detectability indicate that
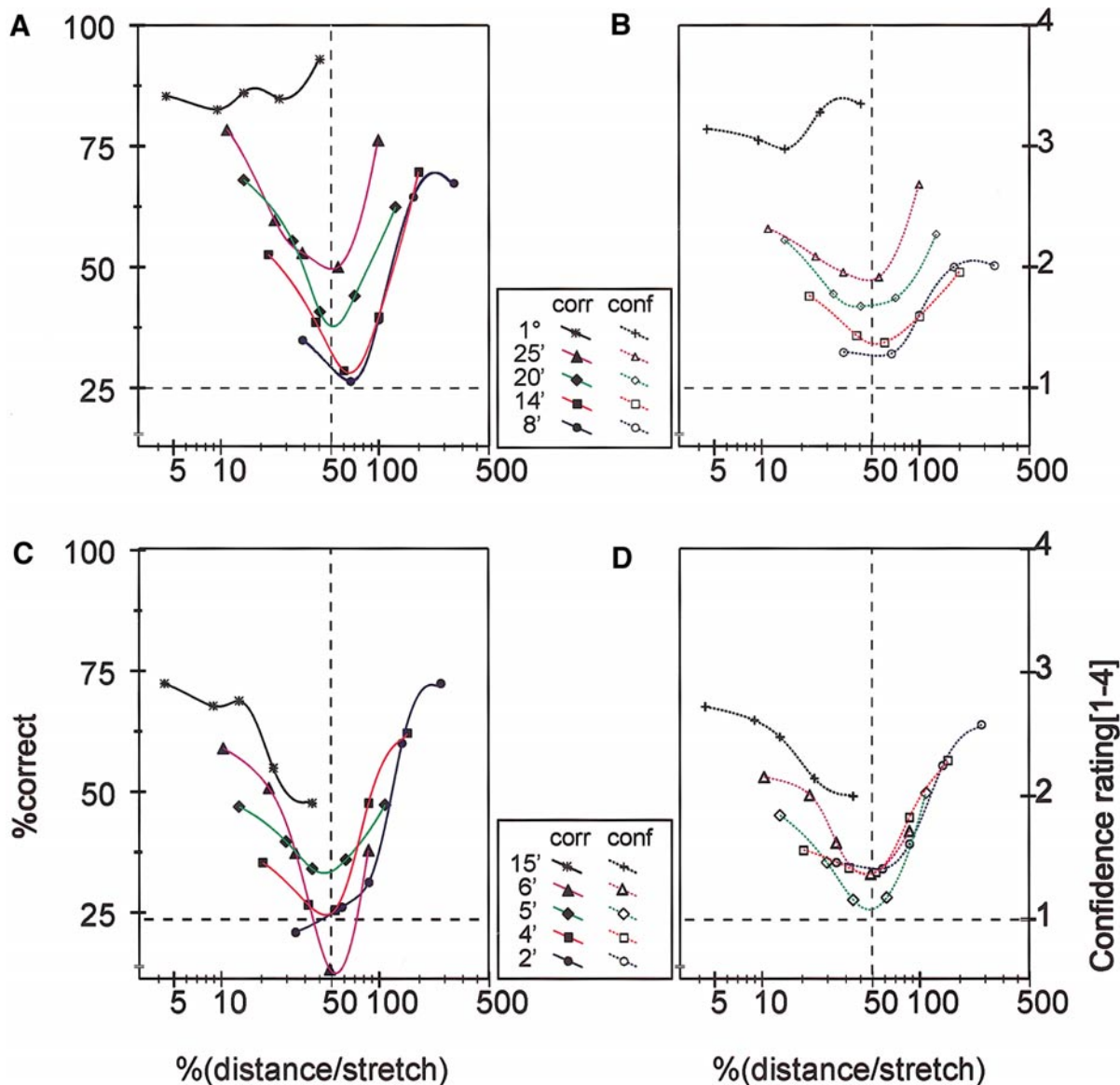
**FIG. 3.** Performance in psychophysical experiment I and II: Behavioral mean responses of 10 subjects (PI: 4; PII: 6) to 50 stimulus conditions (PI: 25; PII: 25). Mean performances for PI (A) and PII (C) are plotted in solid symbols for each stimulus condition. Performances in conditions of equal dot stretch are connected with solid lines that are fitted by a spline function (stiffness: 0.25). Dot vicinity is given on the abscissa expressed in percent ratio of dot distance to motion stretch (vicinity ratio). Mean subjective confidence ratings for PI (B) and PII (D) are plotted in open symbols (and dotted lines) for each stimulus condition and refer to the right ordinate. The minimal and maximal values of left and right ordinate systems were aligned (performance 25 to 100% with confidence ratings 1 to 4). Confidence ratings were correlated to performance and were significant for all conditions that exceeded the chance level significantly (not shown). The stimulus conditions for the fMRI-b experiment were selected from the psychophysical functions shown in (A).

**FIG. 4.** Group results and single subject results of fMRI-a experiment. (A) Three different statistical maps were superimposed on a cortical reconstruction of an MNI-template brain and are shown from three different views (left, posterior, right). Regions contributing significantly to the GLM model are shown in green ($F > 4$, $P < 0.0005$, uncorrected). Maps for linear trend contrast were calculated from the GLM. Regions that responded with increasing amplitude for increasing angles between motion trajectories are shown with red-to-yellow colors. Regions that respond with decreasing amplitudes for increasing angles are shown with blue-to-cyan colors. (B) Activation profiles for the regions shown in A provided for left (LH) and right (RH) hemisphere (colors of the profile match to the color of the regions in A). Beta weights were taken from the GLM and used as measure for central tendency. Bars show the beta weights and the standard error for the corresponding conditions: TM-0°, TM-23°, TM-62°, TM-90°, TM-118°, TM-180°. Correlation between beta weights and angles are given in Table 1. The regression line and the 95% confidence interval of the regression (between beta weights and angles) are indicated for each activation profile in red. (C) Contrast maps of the group data are shown again on a flattened representation of the right cortical sphere and can be compared to single subject data. (D) Single subject contrast maps on flattened representations of the subjects right cortical sheet. Regions that show increasing activity with increasing angles are shown in colors red-to-yellow. Regions that decrease with increasing angles are shown in blue-to-cyan colors. Field sign maps (green and blue) are derived from individual retinotopic mapping and indicate the extensions of the early visual areas (green: V1, V3, VP; blue: V2, V3a, V4). Gray scale contours reflect the tissue curvature.
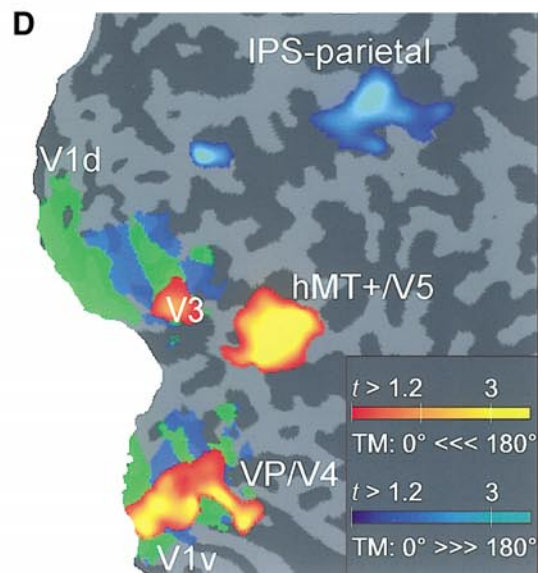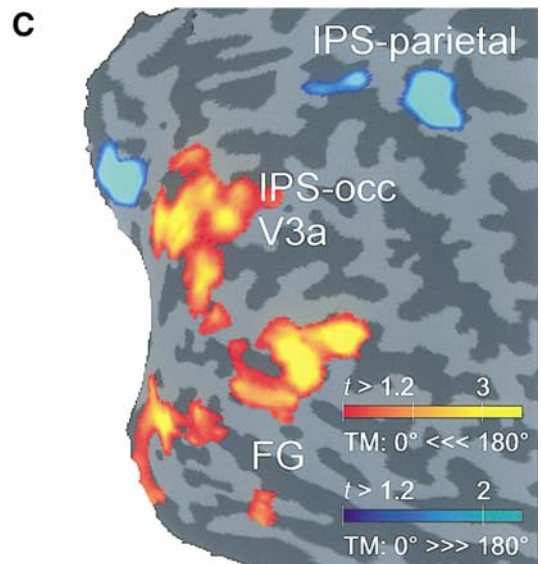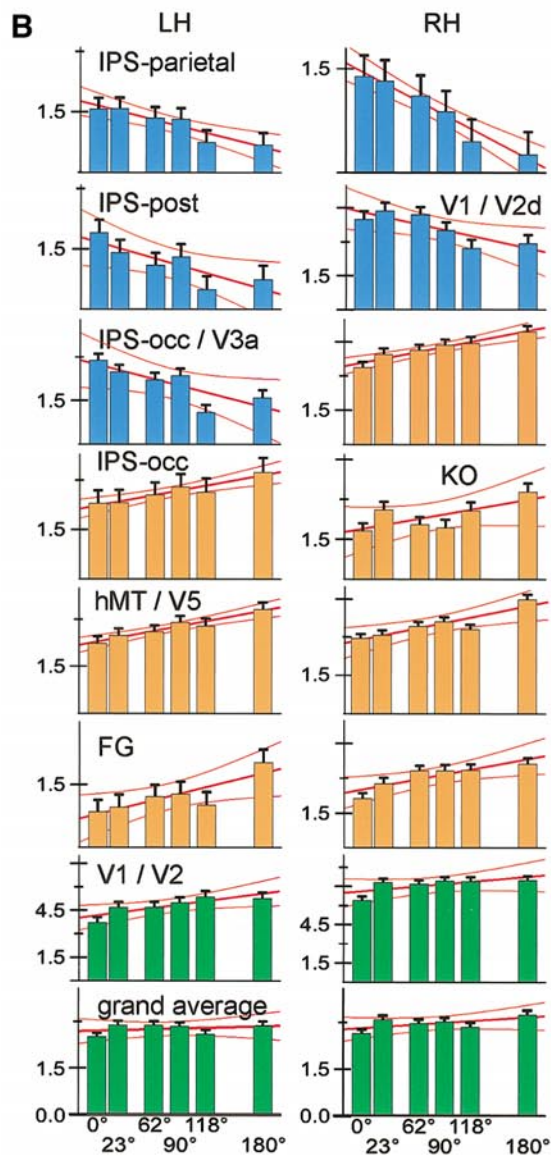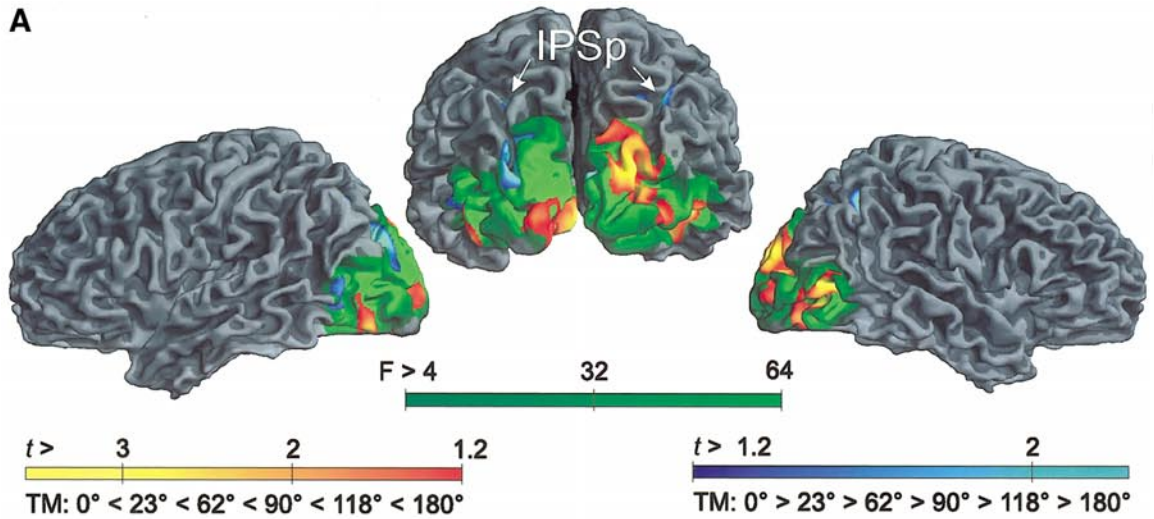
motion transparency is perceived best if dot distance and dot stretch are at the upper end of the tested range. Thus, both parameters had to be considered together for quantification of stimulus conditions. When the vicinity ratio, the ratio of dot distance over dot stretch, was smaller than 40%, the dot pairs were perceived as smeared but oriented lines that form a texture and stimuli appeared as nontransparent and non moving. Nevertheless, different directions of motion were detected indirectly because they produced smeared lines of different orientation. Thus, target regions popped out due to orientation contrast. Perceptual smearing increased with decreasing dot distance. Accordingly, target detection improved with decreasing dot distances for stimuli with a distance ratio <40% (note the descending slopes of solid lines in the left sections of Figs. 3a and 3b).

Target detection was poorest at a vicinity ratio of 50%. In this condition subjects reported to perceive a texture field of incoherently flickering, stationary dots. Confidence ratings (dotted lines in Figs. 3a and 3b) and performance (solid lines in Figs. 3a and 3b) clearly indicate that motion transparency and direction of local motion vectors were neither perceived (confidence rating) nor detected (forced-choice performance). Performance, confidence rating and the correlation between performance and confidence were minimal and not significant ($P > 0.05$; for all conditions with stretches < 15'). Consequently, we used this stimulus configuration as our nontransparent control condition (NT) in the subsequent fMRI-b study. (On a long exposure photograph, stimuli with a ratio of 50% appear as a texture of equally spaced double line segments whose stretch is twice as long as their distance.)

When vicinity ratios increase above 80%, performance increases again (compare ascending solid slopes in the right sections of Figs. 3a and 3b). Dots moving in the same direction are grouped perceptually and separated from nearby dots that move in the opposite direction. Subjects now report to perceive transparent moving surfaces. With increasing vicinity ratios, perception of transparency increases further and opponent moving dots appear as entirely unrelated. To induce a robust percept of transparent motion in the fMRI-b experiment we selected for the transparent motion condition (TM) a vicinity ratio of 130%. We settled for this value because with much higher ratios, e.g., 300%, the texture becomes homogeneous and dots do no longer appear in clusters.

During the fMRI-b experiment subjects responded correctly in 85% of the TM conditions but performed only at chance level during NT condition. This was consistent with the prior expectation derived from the psychophysical experiments.

In the fMRI-a experiment, subjects reported verbally to have no transparent motion percept in the TM-0° and only a weak percept of transparent motion in the TM-23° condition. In all other conditions the percept of transparent moving surfaces was vivid (TM-62°, TM-90°, TM-118°, TM-180°).

*Experiment fMRI-a*

*Group analyses.* We found areas hMT+/V5, right IPS-occ/V3a, V1/V2, and FG-collateral to increase with increasing angles between the two motion trajectories (linear trend contrast: TM-0° < TM-23° < TM-62° < TM-90° < TM-118° < TM-180°). Corresponding positive contrast values are shown in Fig. 4 with red-to-yellow colors. The most significant linear trend ($r = 0.97$, $P = 0.002$) was found in hMT+/V5 of the left hemisphere, followed by right IPS-occ ($r = 0.96$, $P = 0.002$), left IPS-occ ($r = 0.95$, $P = 0.004$) and right hMT+/V5 ($r = 0.90$, $P = 0.02$). For further details, see Table 1. In the contrary, activity in parietal IPS, left post-IPS-occ, and right dorsal V1/V2 decreased with increasing angels (Fig. 4, blue-to-cyan colors, Table 1). Other occipital regions responded equally well to the different conditions. A grand average of all activated regions ($F > 4$, $P < 0.0005$, uncorrected) showed no linear trend (Fig. 4, bottom).

*Single subject analysis.* For each subject, seperate contrast maps were calculated for the increase and for the decrease of activity with increasing angle between the two motion trajectories. Subsequently, maps were compared to the area boundaries as shown for one subject in Fig. 4d. Early visual areas (V1, V2, V3, VP, V3a) were delineated by retinotopic mapping of the vertical and horizontal meridians using field sign maps (Engel *et al.,* 1994; Sereno *et al.,* 1995). As in the group analysis, area hMT+/V5 showed the strongest increase of activity with increasing angle. For the subject shown, the response increase was more widespread in ventral retinotopic visual areas (V1v, V2v, VP/V4) than in dorsal early visual areas. A negative linear trend— decreasing activity with increasing angles—was observed in IPS-parietal and posterior IPS.

*Experiment fMRI-b*

*Group analyses.* The main results of the group analysis are summarized in Fig. 5 and Table 2 and show regions of enhanced activation across seven subjects. To be considered in further analyses an area had to be correlated significantly with reference functions for either TM (transparent motion) or NT (nontransparent) or both (multiple $R > 0.4$, $P < 0.00001$, corrected) and had to exceed a minimal size of $4 \times 4 \times 4$ mm[3] (Fig. 5). Most of the occipital, the occipitotemporal and occipitoparietal cortex was activated equally during NT and TM conditions (yellow regions in Fig. 5). Differential activation levels under NT and TM conditions were only found in higher motion responsive areas and in somato-motor areas, the transparent motion condition being more effective in the human motion

## TABLE 1

### Activated Regions from fMRI-a Experiment

| | Left | | | | | | | | | | Right | | | | | | | | | |
| | Talairach | | | Vol | GLM (full model) | | Contrast | | $r_{(beta * angle)}$ | | Talairach | | | Vol | GLM (full model) | | Contrast | | $r_{(beta * angle)}$ | |
| Cortical region | x | y | z | mm³ | F | P (corr.) | t | P | r | P | x | y | z | mm³ | F | P (corr.) | t | P | r | P |
|---|---|---|---|---|---|---|---|---|---|---|---|---|---|---|---|---|---|---|---|---|
| IPS parietal | −36 | −42 | 41 | 8³ | 12 | 0.00001 | −3.1 | 0.002 | −0.93 | 0.006 | | | | | | | | | | |
| IPS-post | −27 | −64 | 41 | 7³ | 9 | 0.00001 | −3.2 | 0.001 | −0.83 | 0.05 | 26 | −53 | 42 | 11³ | 14 | 0.00001 | −4.0 | 0.0001 | 0.97 | 0.001 |
| V2d cuneus | | | | | | | | | | | 3 | −78 | 16 | 10³ | 57 | 0.00001 | −4.1 | 0.0001 | −0.83 | 0.05 |
| V3a | −24 | −77 | 22 | 13³ | 46 | 0.00001 | −5.3 | 0.0001 | −0.81 | 0.05 | 18 | −88 | 23 | 14³ | 142 | 0.00001 | 3.5 | 0.0005 | 0.96 | 0.002 |
| IPS-occ/V7 | −8 | −84 | 30 | 7³ | 23 | 0.00001 | 2.4 | 0.02 | 0.95 | 0.004 | | | | | | | | | | |
| KO | | | | | | | | | | | 30 | −88 | 4 | 7³ | 34 | 0.00001 | 2.8 | 0.005 | 0.70 | 0.1 |
| HMT+/V5 | −48 | −75 | −2 | 10³ | 81 | 0.00001 | 3.8 | 0.001 | 0.97 | 0.002 | 40 | −70 | 3 | 14³ | 196 | 0.00001 | 5.8 | 0.00001 | 0.90 | 0.02 |
| FG/collateral | −21 | −53 | −13 | 5³ | 11 | 0.00001 | 2.5 | 0.01 | 0.85 | 0.03 | 19 | −65 | −14 | 11³ | 86 | 0.00001 | 4.7 | 0.000003 | 0.88 | 0.03 |
| V1/V2 calcarinus | −11 | 88 | 1 | 13³ | 92 | 0.00001 | 3.5 | 0.001 | 0.85 | 0.05 | 7 | −79 | 0 | 12³ | 304 | 0.00001 | 3.3 | 0.001 | 0.69 | ns |
| Occ/great avg | −24 | −78 | 6 | 27³ | 224 | 0.00001 | 0.8 | ns | 0.34 | ns | 21 | −79 | 6 | 29³ | 225 | 0.00001 | 0.7 | ns | 0.89 | 0.02 |

*Note.* All regions that are colored in Fig. 4a are listed here and provided with Talairach coordinates, size in cubic millimeter and statistic values for the activity (full model, *F, P*), for specific contrasts (*t, P*) TM-0° < TM-0° < TM-23° < TM-62° < TM-90° < TM-118° < TM-180°, and for the correlation of beta weights to the angles of the conditions. Coordinates as defined by Talairach and Tournoux (1988; x, left-right; y, anterior-posterior origin in anterior commisure; z, inferior-superior). Abbreviations: IPS, intraparietal-sulcus; IPS-post, IPS-posterior section; IPS-occ, occipital part of IPS also known as superior occipital sulcus SOS; KO, kinetic occipital region; hMT+/V5, human motion complex-homologue to monkey mid-temporal region and area V5; FG, fusiform gyrus; Occ/great avg: great average of occipital cortex—cortex based analysis.

complex (hMT+/V5), parts of the fusiform gyrus (FG), in the occipital part of the right intraparietal sulcus (IPS-occ) and around the central sulcus (red in Fig. 5, Table 2). Weaker activity during transparent motion perception was observed in areas VP/KO and around the precentral/mid-frontal sulcus (green in Fig. 5, Table 2).

Visual areas V1, V2, V3a, KO/LOC, and the FEF were identified according to functional and topological criteria (Sunaert *et al.,* 1999; Tootell *et al.,* 1998b), the other areas were classified only according to anatomical criteria (FG, Pre/PostCS, MFG).

Relative modulation of the BOLD signal during TM was expressed as percent signal change relative to NT and tested explicitly with the contrast TM > NT (see Table 2). The amplitude of activation was derived from the beta weights of the group analysis for the selected regions (Table 2). Besides response-related activity in

## TABLE 2

### Activated Regions from fMRI-b Experiment

| | Left | | | size | BOLD | GLM (full model) | | contrast TM > NT | | Right | | | Size | BOLD | GLM (full model) | | Contrast TM > NT | |
| | Talairach | | | | | | | | | Talairach | | | | | | | | |
| Cortical region | x | y | z | Vol | $\frac{TM}{NT}$ | F | P (corr.) | t | P | x | y | z | Vol | $\frac{TM}{NT}$ | F | P (corr.) | t | P |
|---|---|---|---|---|---|---|---|---|---|---|---|---|---|---|---|---|---|---|
| V1/V2 calcarinus | −12 | −86 | −3 | 21³ | 114% | 817 | 0.001 | 3.2 | 0.001 | 3 | −89 | 1 | 21³ | 109% | 578 | 0.001 | 2.5 | 0.01 |
| KO | | | | | | | | | | 35 | −82 | 2 | 11³ | 109% | 141 | 0.001 | 1.4 | ns |
| IPS-occ/V7/V3A | −26 | −71 | 24 | 12³ | 213% | 43 | 0.001 | 5.8 | 0.000001 | 26 | −71 | 28 | 11³ | 769% | 32 | | 5.1 | 0.000001 |
| hMT+/V5 | −40 | −65 | 3 | 13³ | 145% | 174 | 0.001 | 6.3 | 0.000001 | 50 | −56 | 5 | 12³ | 147% | 84 | 0.001 | 5.6 | 0.000001 |
| FG/LO | −44 | −59 | −2 | 13³ | 162% | 157 | 0.001 | 2.5 | 0.02 | 43 | −60 | −6 | 12³ | 196% | 87 | 0.001 | 6.0 | 0.000001 |
| FG/collateral | −30 | −65 | −9 | 10³ | 134% | 164 | 0.001 | 5.3 | 0.000001 | 31 | −63 | −8 | 12³ | 263% | 97 | 0.001 | 4.0 | 0.0001 |
| Angularis | −44 | −51 | 10 | 12³ | 344% | 20 | 0.001 | 5.4 | 0.000001 | 53 | −42 | 19 | 11³ | 214% | 28 | 0.001 | 4.3 | 0.00002 |
| Pre CS | −50 | 2 | 32 | 10³ | 370% | 37 | 0.001 | 3.8 | 0.0002 | 44 | 1 | 40 | 12³ | 213% | 75 | 0.001 | 4.7 | 0.000002 |
| Post CS | | | | | | | | | | 55 | −24 | 32 | 11³ | 310% | 54 | 0.001 | 8.7 | 0.000001 |
| | | | | | | | | | | | | | | | | | | |
| PreCS/FEF/MFG | −47 | 11 | 28 | 11³ | 50% | 21 | 0.001 | −4.0 | 0.00007 | 41 | 25 | 32 | 11³ | 67% | 39 | 0.001 | −2.4 | 0.02 |
| Angularis | −50 | −49 | 35 | 9³ | 51% | 9 | 0.001 | −2.6 | 0.01 | | | | | | | | | |
| VP/KO | −37 | −77 | −5 | 13³ | 75% | 115 | 0.001 | −4.5 | 0.00001 | 25 | −82 | −8 | 11³ | 82% | 283 | 0.001 | −4.7 | 0.00001 |

*Note.* All regions that are colored red or green in Fig. 5 are listed here and provided with Talairach coordinates, size in cubic millimeter and statistic values for the activity (full model, *F, P*) and for the specific contrasts TM > NT (*t, P*). Differential activation is indicated by the percent beta weight of TM relative to NT. (Abbreviation as in Table 1; CS: central sulcus; FEF: frontal eye field).
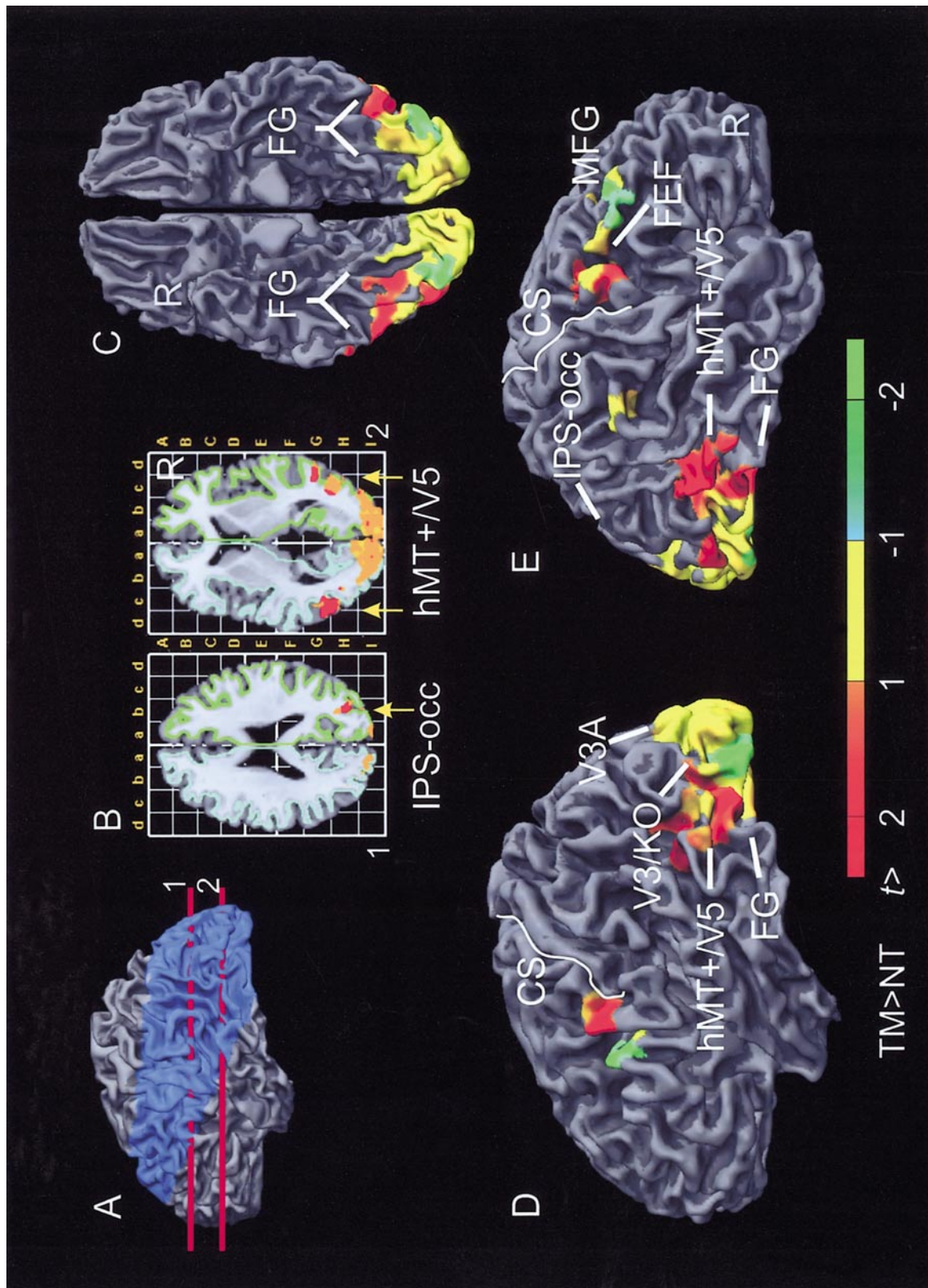
**FIG. 5.** Group analyses of fMRI-b experiment. Group results of seven subjects superimposed onto an individual MNI template brain. Multisubject GLM analyses were performed using a GLM with independent predictors for conditions of TM (transparent motion) and NT (nontransparent). Colored region contribute significantly to the GLM ($F > 4$; $P < 0.005$; uncorrected). Contrast between TM and NT are indicated on separate color scales: More activation during TM than during NT is shown with red-to-yellow colors. More activation during NT than TM is shown with blue-to-cyan colors. Regions with significant contrasts are labeled in the axial slices (B; $z$: +6; +22), in the lateral (D, E) and in the ventral views (C) of the brain surface (see Table 2). The analyses were restricted to the brain region that was commonly imaged in all seven subjects (A: shown in blue). The cortex of the template cerebrum was segmented and reconstructed along the gray-white matter border shown in (B) (blue and green).
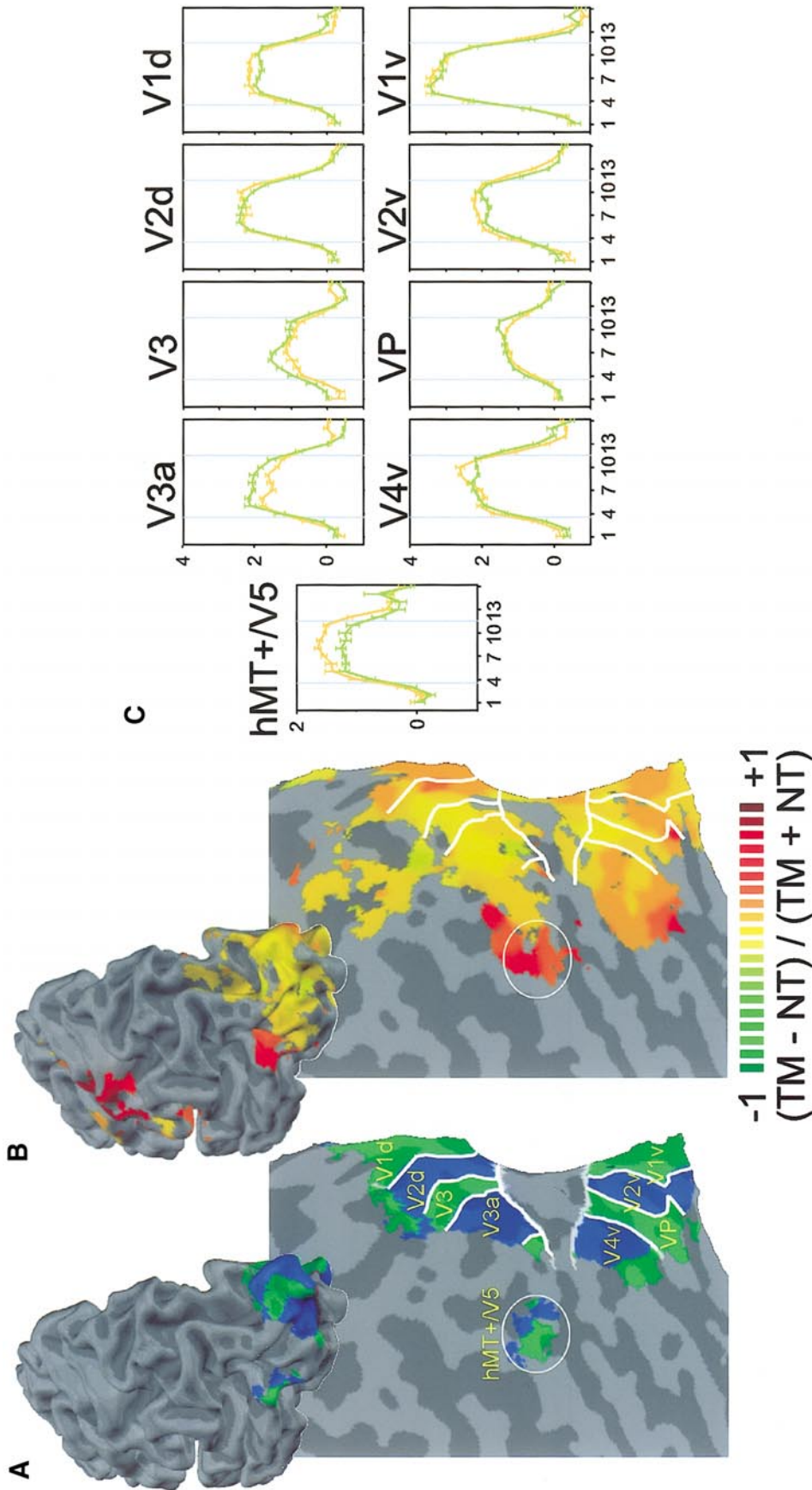
**FIG. 6.** Single subject analyses of fMRI-b. Results of retinotopic mapping and fMRI-b experiment superimposed on a reconstructed (top) and on a flattened representation of the left occipital cortical sheet. Gray scale contours reflect the tissue curvature (dark: concave, light: convex). (A) Field sign maps (green-blue) were derived from the eccentricity and polar angle maps and used to delineate early visual areas (see methods). (B) Relative contribution map ($|TM - NT|/|TM + NT|$) indicates if a region is stronger activated by TM stimuli (red) or by NT stimuli (green) or equally by either stimuli (yellow). (C) Averaged signal time course in early visual areas and hMT+/V5 from the subject shown in A and B for TM (red) and NT (green; small whiskers indicate 1 standard error of the mean).

the central sulcus, the highest contrast values were found in left hMT+/V5 ($t = 6.3$; $P < 0.01$, corrected), followed by right FG ($t = 6.0$; $P < 0.01$, corrected) and right hMT+/V5 ($t = 5.6$; $P < 0.01$, corrected).

*Single subject analyses.* A typical activation pattern from one subject is shown in Fig. 6. The largest regions with highest differential responses to TM were the human motion complex (hMT+/V5), the somatosensory and motor cortex and the frontal eye fields (FEF). Additional regions with less pronounced differential TM activation were observed in the fusiform gyrus, in the right intraparietal sulcus (IPS-occ), and in a subpart of V1. As V1 exhibits slightly inhomogeneous activation in this subject we present two time courses (V1d, V1) that indicate the range of possible profiles. All other subjects showed even less variation in V1. Areas V2, V3, and VP showed also no or only small differences between TM and NT conditions. In this subject only area V3a showed weaker activity during TM. The location of many activated regions could be specified more precisely with regard to retinotopically mapped areas (Fig. 6A). Within the fusiform gyrus (posterior part of the gyrus anterior), a TM sensitive region was found to lay anterior or partly overlapping to area V4v (Lueck *et al.,* 1989; Zeki *et al.,* 1998) and area V8 (Hadjikhani *et al.,* 1998).

IPS-occ is located at the occipital end of the (IPS) were it descends to the superior occipital sulcus (SOS) near the transverse occipital sulcus and anterior to V3A. Because of its anatomically location IPS-occ is likely to correspond to area V7 (Tootell *et al.,* 1998b). In this subject—like in three others—only right presumed V7 showed differential TM activation. Of the remaining three subjects, two showed TM-enhancement in presumed V7 in both hemispheres and one only in the left hemisphere.

*Target related activity.* Group data and single subject data were reanalyzed using a four predictor model (GLM). In this approach predictors specified not only the perceptual condition (TM, NT) but also the hemifield of target presentation (left, right). In each block the targets appeared more frequently (85%) in the left or right lower visual hemifield. Regions that are responsive to the lower visual field (dorsal retinotopic areas V1d, V2d, V3, V3a; Fig. 6c) were inspected closely for signal enhancement during blocks of contralateral target presentations. A left versus right contrast was separately calculated for TM and NT conditions. Neither contrast disclosed an area that exhibited enhanced activation when targets were in the contralateral visual field.

*Eye movements and attention shifts.* We monitored the stability of eye fixation during the fMRI-b experiment with an infrared eye-tracker device in two subjects yielding no differences—within a precision of 1°— between fixation and other conditions (TM or NT).

Even though covert attention shifts (Petit and Haxby, 1999) might occur during the target search in the fMRI-b experiment, it is unlikely that these contributed to the enhanced activity during TM because mean search times were longer during NT trials (87% of the trial time) than during the TM trials (54% of the trial time). Mean search times indicate in percent the time in which no button was pressed with respect to trial duration.

## DISCUSSION

### Psychophysics

Psychophysical experiments revealed that transparent motion is perceived if dot distance exceeds 50% of the motion stretch. This scale-independent result is surprising because one would expect a constant distance value, if transparent motion perception would be a simple consequence of receptive field properties, i.e., averaging of opponent motion vectors at small distances and preserving motion preference at larger distances. Instead of a constant distance value we observed a fix ratio for the tested distances between 0.7′ and 14′. This leads to the quite remarkable conclusion that with increasing motion stretches, more distance is required to render motion transparency.

Qian *et al.* (1994b) proposed a model that incorporates spatial pooling and motion opponency mechanism and seeks to account for the fact that some stimuli consisting of two moving components elicit the perception of motion transparency (like the TM stimulus) while others (like the NT stimulus) do not. In this model, suppressive interactions occur within many small subunits each of which receives inhibitory inputs from detectors tuned to different directions of motion. This suppressive interaction occurs in spatially restricted subunits and prevents TM perception in conditions in which opponent moving dots are in close vicinity and supports TM perception if the distance between opponent moving dots is large.

The results of our psychophysical experiments are difficult to explain by spatially restricted suppression alone. Thus, the length of the motion streaks needs to be considered as an additional variable, requiring extension of the model proposed by Qian. A refined model should incorporate that moving features induce smeared representations owing to the temporal integration of the visual system resulting in the perception of oriented contours. Their orientation can serve as an additional cue to recognize the direction of motion (Geisler, 1999). This combination of complementary motion cues might explain that the ratio between the streak length and streak distance (>50%) rather than distance alone was relevant for motion perception in our experiments. The combination of the two motion cues could take place at stages in the visual processing

stream where both cues are available or it could involve a distributed net of specialized regions.

## Human Motion Complex

The fMRI results suggest that hMT+/V5 is the most important cortical area along the dorsal stream for the integration of local motion cues. Areas of the dorsal stream were more active if the local motion cues were perceptually integrated into coherently moving surfaces (fMRI-b). In addition we found that activation was stronger, when two transparent surfaces rather than one single surface were perceived (fMRI-a). Activity increased with the angle between the two motion trajectories. As suggested by animal experiments (Treue *et al.,* 2000), this increasing activity could be related to the recruitement of two neuronal populations that largely overlap for small angles (lower activity) and exhibit less overlap for large angles (high activity).

## Decreasing Activity for Increasing Angles

Interestingly, parietal-IPS showed the reverse response profile as compared to hMT+/V5 with decreasing activity when the angle between the two motion trajectories increased. This inverse trend might reflect a correlation with the tendency to perform spatial attention shifts. A coherently moving surface (small angles) leads to a single spatial attention shift tendency while two transparently moving surfaces (large angles) reduce this tendency due to mutually cancelling shift directions. This interpretation is consistent with the functional role of putative human LIP (Sereno *et al.,* 2001), which responds with increased activity for remembered target positions.

## Other Visual Areas

Early visual areas showed little differential activation. Higher visual areas of the dorsal (hMT+/V5, V7) and ventral visual stream (FG) showed more differential activation. These areas correspond well to the network of areas that are involved in the reconstruction of 3-D shapes from motion (Naumer *et al.,* 2000).

KO has been reported to respond specifically to motion contours (Orban *et al.,* 1995; Van Oostende *et al.,* 1997; Dupont *et al.,* 1997). Motion contours were produced by the target regions in fMRI-b but they were only perceived in TM stimuli. Activation in presumed KO, however, was not markedly increased by TM stimuli indicating either that motion contours were not extracted from transparent displays at the level of KO or our procedure was not sensitive enough for the detection of such effects. The same holds true for V1, which has also been reported to respond to motion contours (Reppas *et al.,* 1997), but whose activation was not markedly increased by TM stimuli. This agrees with the notion that differently moving dots first need to be integrated into different surfaces at the level of hMT+/V5, before contours can be computed.

Increased activation in the FEF around the somatosensory and motor cortex was seen in fMRI-b during conditions of TM and is most likely related to the task and the response, as it is not seen in the fMRI-a experiment when no responses were required. In agreement with this hypothesis, this frontal activation was more pronounced in the hemisphere contralateral to the response hand. The reason for the differential enhancement of this motor related activity is that response frequency was 60% higher in the TM than in the NT condition.

## CONCLUSION

Human MT+/V5 responded to subtle changes of parameters relevant for the perception of transparent motion and is therefore identified as an important motion integration site in the human brain. This finding is in perfect agreement with single cell recordings from monkey MT (Qian and Andersen, 1994; Heeger *et al.,* 1999) and previous fMRI results (Heeger *et al.,* 1999). In addition psychophysical testing revealed new spatio-temporal interactions relevant for transparent motion perception and furthermore a network of areas comprising of region IPS-occ (presumed V7), and a region in the FG that responded also well to transparent motion and seemed to be tightly linked to the response pattern of hMT+/V5. In contrast parietal-IPS (presumed human LIP) responded stronger for coherent motion and less for transparent motion indicating a possible involvement in coding coherent spatial cues. These new findings are compatible with the idea that these regions (V7, FG) benefit from or participate in the integration process accomplished at the level of hMT+/V5.

## ACKNOWLEDGMENTS

## REFERENCES

Adelson, E. H., and Movshon, J. A. 1982. Phenomenal coherence of moving visual patterns. *Nature* **300:** 523–525.

Andersen, G. J. 1989. Perception of three-dimensional structure from optic flow without locally smooth velocity. *J. Exp. Psychol. Hum. Percept. Perform.* **15:** 363–371.

Boynton, G. M., Engel, S. A., Glover, G. H., and Heeger, D. J. 1996. Linear systems analysis of functional magnetic resonance imaging in human V1. *J. Neurosci.* **16:** 4207–4221.

Dierks, T., Linden, D. E. J., Jandl, M., Formisano, E., Goebel, R., Lanfermann, H., and Singer, W. 1999. Activation of Heschl's gyrus during auditory hallucinations. *Neuron* **22:** 615–621.

Dupont, P., De Bruyn, B., Vandenberghe, R., Rosier, A. M., Michiels, J., Marchal, G., Mortelmans, L., and Orban, G. A. 1997. The kinetic occipital region in human visual cortex. *Cereb. Cortex* **7:** 283–292.

Engel, S. A., Rumelhart, D. E., Wandell, B. A., Lee, A. T., Glover, G. H., Chichilnisky, E.-J., and Shadlen, M. N. 1994. fMRI of human visual cortex. *Nature* **369:** 525.

Geisler, W. S. 1999. Motion streaks provide a spatial code for motion direction. *Nature* **400:** 65–69.

Gibson, E. J., Gibson, J. J., Smith, O. W., and Flock, H. 1959. Motion parallax as a determinant of perceived depth. *J. Exp. Psychol.* **58:** 40–51.

Goebel, R., Khorram-Sefat, D., Muckli, L., Hacker, H., and Singer, W. 1998. The constructive nature of vision: Direct evidence from functional magnetic resonance imaging studies of apparent motion and motion imagery. *Eur. J. Neurosci.* **10:** 1563–1573.

Hadjikhani, N., Liu, A. K., Dale, A. M., Cavanagh, P., and Tootell, R. B. H. 1998. Retinotopy and color sensitivity in human visual cortical area V8. *Nat. Neurosci.* **1:** 235–241.

Heeger, D. J., Boynton, G. M., Demb, J. B., Seidemann, E., and Newsome, W. T. 1999. Motion opponency in visual cortex. *J. Neurosci.* **19:** 7162–7174.

Kolb, F. C., and Braun, J. 1995. Blindsight in normal observers. *Nature* **377:** 336–338.

Krauskopf, J., and Farell, B. 1990. Influence of colour on the perception of coherent motion. *Nature* **348:** 328–331.

Kriegeskorte, N., and Goebel, R. 2001. An efficient algorithm for topologically correct segmentation of the cortical sheet in anatomical MR volumes. *NeuroImage* **14:** 329–346.

Linden, D. E. J., Kallenbach U., Heinecke, A., Singer, W., and Goebel, R. 1999. The myth of upright vision. A psychphysical and functional imaging study of adaptation to inverting spectacles. *Perception* **28:** 469–481.

Lueck, C. J., Zeki, S., Friston, K. J., Deiber, M. P., Cope, P., Cunningham, V. J., Lammertsma, A. A., Kennard, C., and Frackowiak, R. S. 1989. The colour centre in the cerebral cortex of man. *Nature* **340:** 386–389.

Mulligan, J. B. 1992. Anisotropy in an ambiguous kinetic depth effect. *J. Opt. Soc. Am. [A]* **9:** 521–529.

Naumer, M., Bonte, M., Grether, M., Muckli, L., Engel, A., Zanella, F. E., Singer, W., and Goebel, R. 2000. Three-dimensional structure-from-motion activates shape-specific areas in the ventral visual processing stream. *NeuroImage* **11**(5): S691.

Orban, G. A., Lagae, L., Raiguel, S., Xiao, D., and Maes, H. 1995. The speed tuning of medial superior temporal (MST) cell responses to optic-flow components. *Perception* **24:** 269–285.

Petit, L., and Haxby, J. V. 1999. Functional anatomy of pursuit eye movements in humans as revealed by fMRI. *J. Neurophysiol.* **82:** 463–471.

Qian, N. 1997. Binocular disparity and the perception of depth. *Neuron* **18:** 359–368.

Qian, N., and Andersen, R. A. 1994. Transparent motion perception as detection of unbalanced motion signals. II. Physiology. *J. Neurosci.* **14:** 7367–7380.

Qian, N., Andersen, R. A., and Adelson, E. H. 1994a. Transparent motion perception as detection of unbalanced motion signals. I. Psychophysics. *J. Neurosci.* **14:** 7357–7366.

Qian, N., Andersen, R. A., and Adelson, E. H. 1994b. Transparent motion perception as detection of unbalanced motion signals. III. Modeling. *J. Neurosci.* **14:** 7381–7392.

Reppas, J. B., Niyogi, S., Dale, A. M., Sereno, M. I., and Tootell, R. B. 1997. Representation of motion boundaries in retinotopic human visual cortical areas. *Nature* **388:** 175–179.

Sereno, M. I., Pitzalis, S., and Martinez, A. 2001. Mapping of contralateral space in retinotopic coordinates by a parietal cortical area in humans. *Science* **294:** 1350–1354.

Sereno, M. I., Dale, A. M., Reppas, J. B., Kwong, K. K., Belliveau, J. W., Brady, T. J., Rosen, B. R., and Tootell, R. B. 1995. Borders of multiple visual areas in humans revealed by functional magnetic resonance imaging. *Science* **268:** 889–893.

Snowden, R. J., Treue, S., Erickson, R. G., and Andersen, R. A. 1991. The response of area MT and V1 neurons to transparent motion. *J. Neurosci.* **11:** 2768–2785.

Sunaert, S., Van Hecke, P., Marchal, G., and Orban, G. A. 1999. Motion-responsive regions of the human brain. *Exp. Brain Res.* **127:** 355–370.

Talairach, J., and Tournaux, P. 1988. *Co-planar Stereotaxic Atlas of the Human Brain.* Thieme, New York, NY.

Tootell, R. B. H., Hadjikhani, N. K., Mendola, J. D., Marrett, S., and Dale, A. M. 1998. From retinotopy to recognition: fMRI in human visual cortex. *Trends Cogn. Sci.* **2:** 174–183.

Treue, S., Hol, K., and Rauber, H. J. 2000. Seeing multiple direction of motion-physiology and psychophysics. *Nat. Neurosci.* **3:** 270–276.

Van Oostende, S., Sunaert, S., Van Hecke, P., Marchal, G., and Orban, G. A. 1997. The kinetic occipital (KO) region in man: An fMRI study. *Cereb. Cortex* 690–701.

Wallach, H., and O'Connell, D. N. 1953. The kinetic depth effect. *J. Exp. Psychol.* **45:** 205–217.

Zeki, S., McKeefry, D. J., Bartels, A., and Frackowiak, R. S. 1998. Has a new color area been discovered? *Nat. Neurosci.* **1:** 335–336.